MOLECULAR AND CELLULAR BIOLOGY, Oct. 1996, p. 5313–5327 Vol. 16, No. 10
0270-7306/96/$04.00+0

The p160 RhoA-Binding Kinase ROKα Is a Member of a Kinase Family and Is Involved in the Reorganization of the Cytoskeleton

THOMAS LEUNG,[1] XIANG-QUN CHEN,[1] EDWARD MANSER,[1] AND LOUIS LIM[1,2]*

Glaxo-IMCB Group, Institute of Molecular & Cell Biology, National University of Singapore, Singapore 119260, Singapore,[1] and Institute of Neurology, London WC1N 1PJ, United Kingdom[2]

Received 27 March 1996/Returned for modification 14 May 1996/Accepted 4 July 1996

The GTPase RhoA has been implicated in various cellular activities, including the formation of stress fibers, motility, and cytokinesis. We recently reported on a p150 serine/threonine kinase (termed ROKα) binding RhoA only in its active GTP-bound state and on its cDNA; introduction of RhoA into HeLa cells resulted in translocation of the cytoplasmic kinase to plasma membranes, consistent with ROKα being a target for RhoA (T. Leung, E. Manser, L. Tan, and L. Lim, J. Biol. Chem. 256:29051–29054, 1995). Reanalysis of the cDNA revealed that ROKα contains an additional N-terminal region. We also isolated another cDNA which encoded a protein (ROKβ) with 90% identity to ROKα in the kinase domain. Both ROKα and ROKβ, which had a molecular mass of 160 kDa, contained a highly conserved cysteine/histidine-rich domain located within a putative pleckstrin homology domain. The kinases bound RhoA, RhoB, and RhoC but not Rac1 and Cdc42. The Rho-binding domain comprises about 30 amino acids. Mutations within this domain caused partial or complete loss of Rho binding. The morphological effects of ROKα were investigated by microinjecting HeLa cells with DNA constructs encoding various forms of ROKα. Full-length ROKα promoted formation of stress fibers and focal adhesion complexes, consistent with its being an effector of RhoA. ROKα truncated at the C terminus promoted this formation and also extensive condensation of actin microfilaments and nuclear disruption. The proteins exhibited protein kinase activity which was required for stress fiber formation; the kinase-dead ROKαK112A and N-terminally truncated mutants showed no such promotion. The latter mutant instead induced disassembly of stress fibers and focal adhesion complexes, accompanied by cell spreading. These effects were mediated by the C-terminal region containing Rho-binding, cysteine/histidine-rich, and pleckstrin homology domains. Thus, the multidomained ROKα appears to be involved in reorganization of the cytoskeleton, with the N and C termini acting as positive and negative regulators, respectively, of the kinase domain whose activity is crucial for formation of stress fibers and focal adhesion complexes.

In mammals, the Ras-related Rho subfamily includes RhoA, -B, and -C, Rac1 and -2, and Cdc42, which play pivotal roles in cytoskeletal control and cell morphology. RhoA has been implicated in stress fiber formation (33, 34), whereas Rac1 (36) and Cdc42 (15, 29) are involved in lamellipodial and filopodial formation, respectively. Fibroblasts injected with these GTPases display a set of distinctive morphological changes, suggestive of probable hierarchy in the order Cdc42, Rac, and Rho. These changes demand a high level of flexibility in the dynamic reorganization of actin microfilaments in cells. RhoA, -B, and -C have about 85% identity and appear to have different cellular localizations (1). Although their exact roles in cells have not been clearly defined, these GTPases have been implicated in a variety of cellular activities either directly by overexpression of wild-type and mutant forms or indirectly by inhibiting their functions with toxins such as the *Clostridium botulinum* C3 transferase. RhoA has been shown to affect morphology (30), cell motility (39), cytokinesis (14), tumor progression (31, 32), and apoptosis (12). RhoB, which exhibits a cell cycle-dependent expression pattern, has an effect on cell transformation (42). The morphological effect of RhoA on actin-containing cytoskeletal structures (36, 38) appears to be cell type specific. Thus, although in most cells, including fibroblasts, the major effect of RhoA is formation of stress fibers, membrane ruffling has also been observed in other cell types (28).

Biochemically, the targets of the Rho GTPases which initiate these phenotypic changes remain largely uncharacterized. The use of specific kinase inhibitors has shown that the pathways leading to formation of stress fibers and of focal adhesion complexes are distinct; they also implicate the possible involvement of kinases, especially downstream tyrosine kinases, in the formation of focal adhesions (35). RhoA is also involved in activating phosphatidylinositol 3-kinase in Swiss 3T3 cells and in human platelet cytosolic extracts (43) and possibly in the activation of phosphatidylinositol 5-kinase (6). In rat liver membranes, RhoA also has a role in the activation of membrane-associated phospholipase D, although direct interaction between the two has not been demonstrated (3). More recently, RhoA has been implicated in the serum-responsive factor-linked signalling pathway (10), while Cdc42 and Rac have been linked to the mitogen-activated protein kinase c-JNK signalling pathway (7, 25). These nuclear events and the identification of kinase targets for Cdc42 and Rac (21, 22) support the notion that the GTPases are participants in distinctive kinase cascades. We have recently isolated a serine/threonine kinase, ROKα (Rho-associated kinase), which responds to activated RhoA by translocating from the cytoplasm to the plasma membranes (18). We now report that the cDNA for ROKα encodes an additional N-terminal region compared with that previously reported (18) and that ROKα is a member

* Corresponding author. Mailing address: Glaxo-IMCB Group, Institute of Molecular & Cell Biology, National University of Singapore, Kent Ridge, Singapore 119260, Singapore. Phone: (65) 772-6167. Fax: (65) 774-0742.

A

ROKα

MPGAPEAAAG DGAGAGRQRK LEALIRDPRS PINVESLLDG LNSLVLDLDF PALRKNKNID 60
NFLNRYEKIV KKIRGLQ**MKA EDYDVVKVIG RGAFGEVQLV RHKASQKVYA MKLLSKFEMI** 120
KRSDSAFFWE ERDIMAFANS PWVVQLFCAF QDDRYLYMVM EYMPGGDLVN LMSNYDVPEK 180
WAKFYTAEVV LALDAIHSMG LIHRDVKPDN MLLDKHGHLK LADFGTCMKM DETGMVHCDT 240
AVGTPDYISP EVLKSQGGDG YYGRECDWWS VGVFLFEMLV GDTPFYADSL VGTYSKIMDH 300
KNSLCFPEDT EISKHAKNLI CAFLTDREVR LGRNGVEEIK SASFFKNDQW NWDNIRETAA 360
PVVPELSSDI DSSNFDDIED DKGDVETFPI PKAFVGNQLP FIGFTYFREN LLLSDSPPCR 420
ENDAIQTRKS EESQEIQKKL YALEEHLSSE VQAKEELEQK CKSINTRLEK TAKELEEEIT 480
FRKNVESTLR QLEREKALLQ HKNAEYQRKA DHEADKKRNL ENDVNSLKDQ LEDLKKRNQS 540
SQISTEKVNQ LQKQLDEANA LLRTESDTAA RLRKTQAESS KQIQQLESNN RDLQDKNCLL 600
ETAKLKLEKE FINLQSALES ERRDRTHGSE IINDLQGRIS GLEEDLKTGK TLLAKVELEK 660
RQLQEKLTDL EKEKSNMEID MTYQLKVIQQ SLEQEEAEHK TTKARLADKN KIYESIEEAK 720
SEAMKEMEKK LLEERSLKQK VENLLLEAEK RCSILDCDLK QSQQKLNELL KQKDVLNEDV 780
RNLTLKIEQE TQKRCLMQND LKMQTQQVNT LKMSEKQIKQ ENNHLMEMKM NLEKQNAELR 840
KERQDADGQM KELQDQLEAE QYFSTLYKTQ VRELKEENEE KTKLCKELQQ KKQDLQDERD 900
SLAAQLEITL TKADSEQLAR SIAEEQYSDL EKEKIMKELE IKEMMARHKQ ELTEKDATIA 960
SLEETNR**TLT SDVANLANEK EELNNKLKDT QEQLSKLKDE EISAAAIKAQ FEKQLLTERT** 1020
LKTQAVNKLA EIMNRKEPVK RGSDTDVRRK EKENRKLHME LKSEREKLTQ QMIKYQKELN 1080
EMQAQIAEES QIRIELQMTL DSKDSDIEQL RSQLQALHIG MDSSSIGSGP GDAEPDDGFP 1140
ES**RLEGWLSL PVRNNTKKFG WVKKYVIVSS KKILFYDSEQ DKEQSNPYMV LDIDKLFHVR** 1200
PVTQTDVYRA DAKEIPRIFQ ILYANEGESK KEPEFPVEPV GEKSNYICHK GHEFIPTLYH 1260
FPTNCEACMK PLWHMFKPPP ALECSRCHIK CHKDHMDKKE EIIAPCKVYY DISSAKNLLL 1320
LANSTEEQQK WVSRLVKKIP KKPPAPDPFA RSSPRTSMKI QQNQSIRRPS RQLAPNKPS. 1379

ROKβ

MSTGDSFETR FEKIDNLLRD PKSEVNSDCL LDGLDALVYD LDFPALRKNK NIDNFLSRYK 60
DTINKIRDLR **MKAEDYEVVK VIGRGAFGEV QLVRHKSTRK VYAMKLLSKF EMIKRSDSAF** 120
FWEERDIMAF ANSPWVVQLF YAFQDDRYLY MVMEYMPGGD LVNLMSNYDV PEKWARFYTA 180
EVVLALDAIH SMGFIHRDVK PDNMLLDKSG HLKLADFGTC MKMNKEGMVR CDTAVGTPDY 240
ISPEVLKSQG GDGYYGRECD WWSVGVFLYE MLVGDTPFYA DSLVGTYSKI MNHKNSLTFP 300
DDNDISKEAK NLICAFLTDR EVRLGRNGVE EIKRHLFFKN DQWAWETLRD TVAPVVPDLS 360
SDIDTSNFDD LEEDKGDEET FPIPKAFVGN QLPFVGFTYY SNRRYLPSAN PSENRSSSNV 420
DKNVQESLQK TIYKLEEQLH NEMQLKDEME QKCRTSNIKL DKIMKELDEE GNQRRNLESA 480
VSQIEKEKML LQHRINEYQR KVEQENEKRR NVENEVSTLK DQLEDLRKAS QSSQLANEKL 540
TQLQKQLEEA NDLLRTESDT AVRLRKSHTE MSKSVSQLES LNRELQERNR MLENSKSQAD 600
KDYYQLQAVL EAERRDRGHD SEMIGDLQAR ITSLQEEVKH LKHNLERVEG ERKEAQDMLN 660
HSEKEKNNLE IDLNYKLKSI QQRLEQEVNE HKVTKARLTD KHQSIEEAKS VAMCEMEKKL 720
KEEREAREKA ENRVVETEKQ CSMLDVDLKQ SQQKLEHLTE NKERLEDAVK SLTLQLEQES 780
NKRILLQSEL KTQAFEADNL KGLEKQMKQE INTLLEAKRL LEFELAQLTK QYRGNEGQMR 840
ELQDQLEAEQ YFSTLYKTQV KELKEEIEEK NRENLRKIQE LQSEKETLST QLDLAETKAE 900
SEQLARGILE EQYFELTQES KKAASRNRQE ITDKDHTVSR LEEANN**ALTK DIELLRKENE** 960
ELNERMRTAE EEYKLKKEEE ISNLKAAFEK NISTERTLKT QAVNKLAEIM NRKDFKIDRK 1020
KANTQDLRKK EKENRKLQLE LNQEREKFNQ MVVKHQKELN DMQAQLVEEC THRNELQMQL 1080
ASKESDIEQL RAKLLDLSDS TSVASFPSAD ETDGNLPVGS ACIPYLFIFY SSSS**RIEGWL** 1140
SVPNRGNIKR YGWKKQYVVV SSKKMLFYND EQDKEQSSPS MVLDIDKLFH VRPVTQGDVY 1200
RAETEEIPKI FQILYANEGE CRKDIEVEPV QQGEKTNFQN HKGHEFIPTL YHFPANCEAC 1260
AKPLWHVFKP PPALECRRCH VKSHRDHLDK KEDLIPPCKV SYDVTSARDM LLLACPQDEQ 1320
KKWVTHLVKK IPKKAPSGFV RASPRTLSTR STANQSFRKV VKNTSGKTS. 1369

FIG. 1. Analysis of ROKα and ROKβ sequences. (A) Predicted amino acid sequence of ROKα and ROKβ. The presumed translation product is indicated in single-letter code. The kinase, RhoA-binding, and putative PH (containing the CRD) domains are in boldface in order of appearance, N to C terminal. The peptide sequence encoded by the initial cDNA sequence of ROKβ obtained by expression screening is underlined. (B) ROKα and ROKβ are members of a kinase family. Multiple alignment of ROKβ and ROKα with other related kinases was performed with the Clustal method (DNASTAR). The kinases include human myotonic dystrophy kinase (DMK; accession number L08835), *Drosophila warts* gene product (Wts; accession number L39837), *Neurospora* cot-1 (accession number P38679), and rat protein kinase Cα (PKCα; accession number P28867). (C) Alignment of PH domains of ROKα and ROKβ with other PH domains from consensus sequences (boldface capital letters) of most commonly occurring amino acids as defined by Musacchio et al. (27). Note the presence of the CRD within the PH domains of the ROKs. (D) Alignment of the CRDs of ROKβ and ROKα with the CRDs of PKCα, Raf-1, and *n*-chimaerin (N-chim). The invariant residues present in most CRDs of this class are in boldface. (E) Diagrammatic representation of the linear sequences of ROKβ and ROKα. The percent identities of different regions, including the Rho-binding domain (BD), are also indicated.

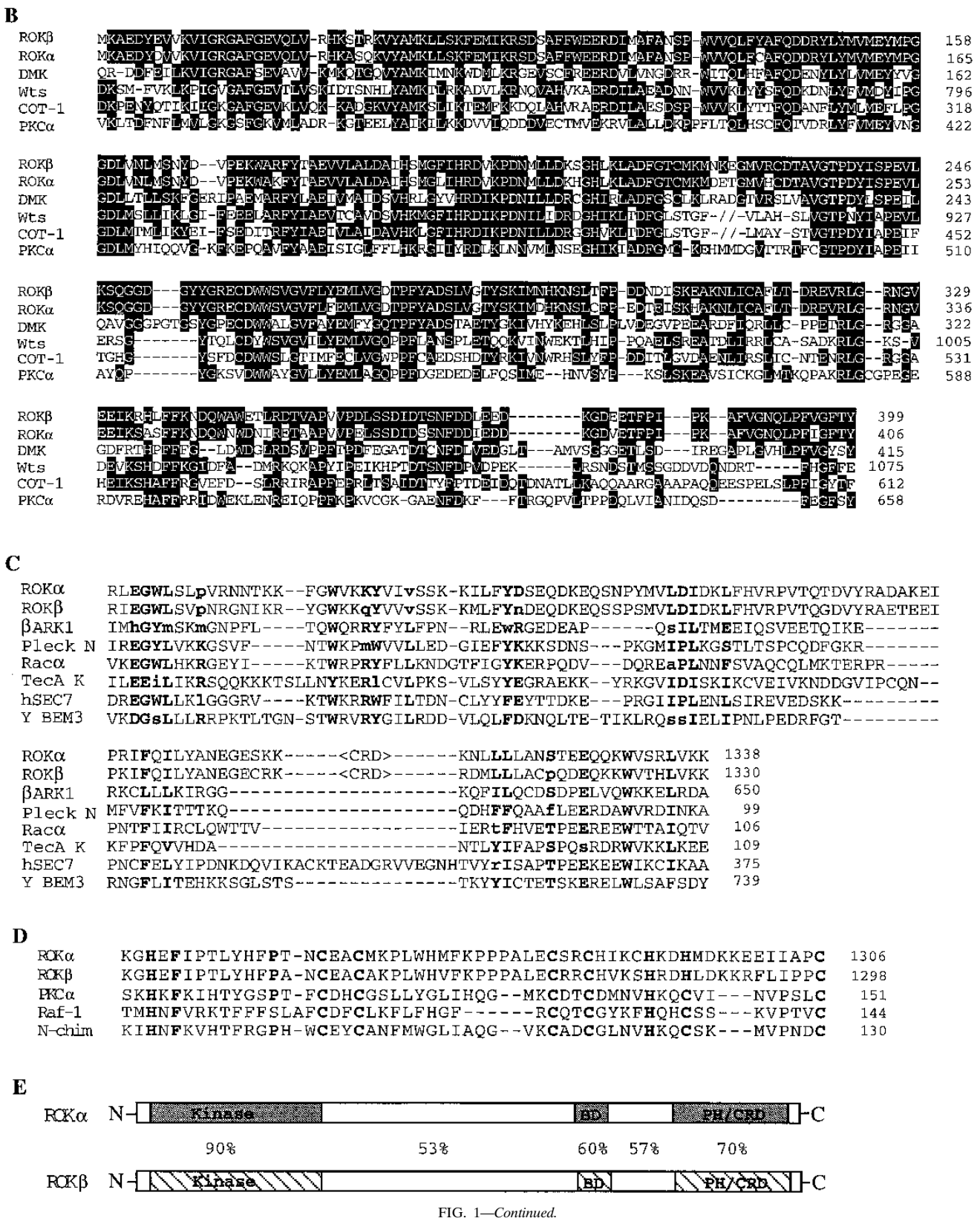

FIG. 1—*Continued.*

of a family of related kinases binding Rho GTPase. Microinjection of an expression vector encoding ROKα results in the formation of stress fibers and focal adhesion complexes in HeLa cells. This effect required both the kinase domain and the N-terminal region and was dependent on kinase activity. Deletion of the N-terminal region resulted in the truncated ROKα being kinase inactive and inducing loss of stress fibers and focal adhesion complexes, accompanied by cell spreading. These effects were dependent on the RhoA binding and PH (pleckstrin homology)/CRD (cysteine/histidine-rich domain) region. Our results indicate that ROKα is a Rho-target kinase which plays a major role in the restructuring of the cytoskeleton.

MATERIALS AND METHODS

Screening of cDNA libraries from rat brain and liver to obtain ROKβ cDNA. Further expression screening of a rat brain cDNA library (Stratagene) by using [γ-^{32}P]GTP-labeled RhoA yielded an additional cDNA clone which was different from our previously isolated ROKα (18). This cDNA fragment (nucleotides [nt] 2203 to 3190), which included the RhoA-binding domain (see Fig. 1 and 3), was used as a probe to screen 500,000 phages from the rat brain cDNA library. Twelve clones were obtained, and overlapping restriction fragments were subcloned into pBluescript for sequencing in both directions, using a Sequenase kit (U.S. Biochemical). The 5′ ends of these clones contained divergent sequences (which lacked DNA encoding the first ~70 amino acids [aa]), possibly as a result of cloning artifacts or differential splicing events in brain tissue. Upon screening a rat liver cDNA library which should contain high levels of ROKβ cDNA, as predicted from the Northern (RNA) analysis (see Fig. 2B), we obtained four overlapping clones encoding full-length ROKβ. The 5′ ends of two of these clones showed significant homology to the 5′ end of ROKα; this enabled us to pinpoint the upstream initiation codon for both ROKα and ROKβ cDNAs.

Protein analysis. Rat brain tissues were obtained by homogenization in extraction buffer containing 50 mM Tris-HCl (pH 8.0), 5 mM $MgCl_2$, 0.1% Triton X-100, 1 mM phenylmethylsulfonyl fluoride, and 1 μg each of aprotinin, pepstatin, and leupeptin per ml. Soluble fractions (150 μg) after centrifugation at 100,000 × *g* for 30 min at 4°C were separated on sodium dodecyl sulfate (SDS)–9% polyacrylamide gels and transferred to nitrocellulose filters for [γ-^{32}P]GTP-RhoA binding assays as described previously (22). Western blot (immunoblot) analyses were performed with polyclonal antibodies raised against the conserved kinase domain of ROKα (aa 112 to 393) and the p21-binding domain of ROKβ (aa 670 to 1027). Specific immunoreactivity was detected by using an ECL kit (Amersham International, Amersham, England).

RNA analysis. Total RNA was obtained by the guanidinium isothiocyanate method and separated on a 1% formaldehyde agarose gel as described previously (16). Poly(A)$^+$ RNA from various rat tissues was purchased from Clontech. After transfer to Hybond filter (Amersham), blots were hybridized with either ^{32}P-labeled ROKα (nt 407 to 1252) or ROKβ (nt 402 to 1266). Blots were exposed to X-ray films and developed after 24 h of exposure. As a control, the same blot was hybridized to a ^{32}P-labeled β-actin cDNA probe (Clontech) and exposed for 4 h.

Expression and purification of fusion proteins for analysis. Glutathione *S*-transferase (GST) fusion proteins of RhoA, RhoA^{V14}, Rac1, and Cdc42Hs were obtained as previously described (20). GST-RhoA^{V14} was further cleaved with thrombin and used at 0.5 μg/μl for microinjection. Human RhoB and RhoC were generated from published sequences (5) by PCR and subcloned in frame into pGEX-2TK vector (Pharmacia) for expression. For expressing the binding domains of the kinases, a *Hha*I-*Hin*dIII fragment of ROKβ (nt 2950 to 3190; encoding aa 947 to 1027) and a *Hin*cII-*Hin*dIII fragment of ROKα (nt 2498 to 3257; encoding aa 809 to 1062) were used to subclone in frame into the pMAL vector (New England Biolabs) for expression. GST-αPAK was obtained as previously described (19). For mutagenesis, ROKα was used as the template for two rounds of PCR using *Taq* polymerase (19). Mutants were subcloned in frame into pMAL vector and fully sequenced. The following primer pairs were used for mutants M1 to M3: for M1, 5′CGCAGTCAGCAGCTGCTTC3′ and 5′GCAA CACTCAAGACTCAAG3′; for M2, 5′GAGTCTCGAGTGTTCGCTCAG3′ and 5′TAGCTGTGAATAAGTTGG3′; and for M3, 5′TAGTCACAGCTTGA GTC3′ and 5′CGTTGGCAGAGATCATG3′. Wild-type and mutant proteins were purified by recommended procedures (New England Biolabs), and 1 μg of these proteins was separated on an SDS–10% polyacrylamide gel for staining and transfer to nitrocellulose filter for binding assays. For determining the binding specificity of the recombinant proteins, fusion proteins (1 μg) with binding domains of ROKα, ROKβ, and αPAK were dotted onto nitrocellulose filters. Filters were blotted with renaturation buffer for 2 h before assaying for binding with various p21s prelabeled with [γ-^{32}P]GTP (22). After three washes with washing buffer, pieces of filters containing the dotted protein were excised for scintillation counting.

Construction of mammalian vectors, cell culture, microinjection, and confocal microscopy. For investigating the effect of overexpression of ROK on mammalian cells, ROKα was expressed under the control of the cytomegalovirus enhancer/promoter in pXJ40 vector (40) which has been modified to include the influenza virus hemagglutinin (HA) peptide recognized by monoclonal antibody (MAb) 12CA5 (Boehringer Mannheim) and a polylinker site. The full-length ROKα construct was made in two steps. First, the sequence encoding the kinase domain (nt 71 to 1556) was obtained by PCR (using primers 5′CGGATCCAA AATGCCCGGCGCCCC3′ and 5′CTCTTTCTAGCTGTCTT3′). The 1.5-kb PCR product was digested with *Bam*HI and cloned into the *Bam*HI-*Sma*I-cut pXJ40 vector. The second stage involved the cloning of the rest of the 3′ sequence to produce a full-length construct (aa 1 to 1379). Likewise, the N-terminally truncated constructs were derived from a subclone of a PCR product (using primers 5′CAGGATCCATGAAAGCAGAAGACTATG3′ and 5′CTCT TTCTAGCTGTCTT3′ to give ROKα$^{78\text{-}498}$). The p21 binding-deficient mutant was obtained by replacing the wild-type *Spe*I-*Nde* region (18) with a mutated region containing the M3 double mutation (NK to TT, aa 1027 and 1028). Deletion mutants were obtained by cloning of restriction fragments from full-length (aa 1 to 1379) and N-terminally truncated (aa 78 to 1379) constructs: *Bam*HI-*Eco*RV (aa 1 to 543), *Bam*HI-*Pvu*II (aa 78 to 398), *Bam*HI-*Spe*I (aa 78 to 970), *Bam*HI-*Xmn*I (aa 1 to 1109 and 78 to 1109), *Bam*HI-*Bgl*I (aa 1 to 1271 and 78 to 1271), *Spe*I-*Sph*I (aa 971 to 1379), and *Xmn*I-*Sph*I (aa 1110 to 1379). All constructs were checked by sequencing, and the production of the correct-size proteins was confirmed by in vitro transcription and translation assay by using a Promega kit and by transient transfection into COS-7 cells. DNAs for RhoA^{N19} and Rac1^{N17} were obtained by PCR mutagenesis and subcloned into pXJ40 vector. *C. botulinum* C3 exoenzyme was purchased from UBI Biochemical.

For microinjection, HeLa cells maintained in minimal essential medium in the presence or absence of 10% fetal bovine serum (FBS) were used. Subconfluent cells plated on coverslips for 48 h were microinjected with the different constructs (50 ng/μl), using an Eppendorf micromanipulator. Two hours after injection, cells were fixed with 4% paraformaldehyde and double stained with tetramethylrhodamine isothiocyanate-phalloidin (1 μg/ml; Sigma) and MAb 12CA5 (anti-HA)-fluorescein isothiocyanate (FITC) (Boehringer Mannheim) or with antivinculin (Sigma) or anti-α-tubulin (Sigma) with FITC-conjugated anti-mouse antibody (Sigma) and rhodamine-conjugated anti-HA (Boehringer Mannheim) essentially as previously described (18). For coinjection experiments, HeLa cells were first injected with C3 toxin (0.2 μg/μl) into the cytoplasm followed by injection of a plasmid construct into the cell nucleus. RhoA^{V14} (0.5 μg/μl) was injected either with mouse immunoglobulin G (0.5 μg/μl) or in combination with C3 toxin. Cells were fixed and double stained with FITC-conjugated anti-mouse antibody and phalloidin after 30 min of incubation. Stained cells were analyzed with an MRC 600 confocal imager.

COS-7 cell transfection, immunoprecipitation, and kinase assay. COS-7 cells grown in Dulbecco modified Eagle medium with 10% FBS were transfected with various HA-tagged DNA constructs (1 μg/ml) with Lipofectamine (Gibco/BRL) according to recommended protocol. At 16 h after transfection, cells were extracted with cell lysis buffer containing 25 mM *N*-2-hydroxyethylpiperazine-*N*′-2-ethanesulfonic acid (HEPES; pH 7.3), 0.3 M NaCl, 1.5 mM $MgCl_2$, 0.2 mM EDTA, 20 mM sodium β-glycerophosphate, 1 mM sodium vanadate, 0.5% Triton X-100, and 5% glycerol. For analysis of expression, extracts (100 μg of protein) were separated on an SDS–12% polyacrylamide gel, transferred to nitrocellulose, and probed with rabbit antibodies against ROKα. For immunoprecipitation studies, extracts (400 μg) were incubated with 5 μl of MAb 12CA5 (Boehringer Mannheim) for 2 h before collection on 25 μl of gammaBind Sepharose (Pharmacia). After a wash with 200 μl of lysis buffer and 400 μl of phosphate-buffered saline (with 0.1% Triton X-100), a kinase reaction was carried out in buffer containing 50 mM HEPES (pH 7.3), 10 mM $MgCl_2$, 2 mM $MnCl_2$, 1 mM dithiothreitol, and 0.05% Triton X-100 with 10 μM [γ-^{33}P]ATP and 5 μg of myelin basic protein (MBP). After 30 min, the reaction was stopped by adding 100 μl of SDS sample buffer. After boiling for 5 min, a fraction (20 μl) of this preparation was run on an SDS–12% polyacrylamide gel and transferred to nitrocellulose filter for autoradiography and probing with a rabbit anti-ROK antiserum.

Nucleotide sequence accession numbers. The cDNA sequences of ROKα and ROKβ are deposited with GenBank under accession numbers U38481 and U61266, respectively.

RESULTS

ROKα is a member of a kinase family. The amino acid sequence of the Rho-binding kinase ROKα that we reported earlier (18) was derived from a cDNA which appeared to start at the first methionine upstream of the kinase domain. Following the observations by Kaibuchi and Narumiya (13a) that cDNAs encoding ROKα-related kinases contained additional amino acid residues at the N terminus, we reanalyzed our ROKα cDNAs. This analysis revealed ROKα cDNA to encode an additional N-terminal 77 amino acid residues. The revised sequence of ROKα containing 1,379 amino acid residues is

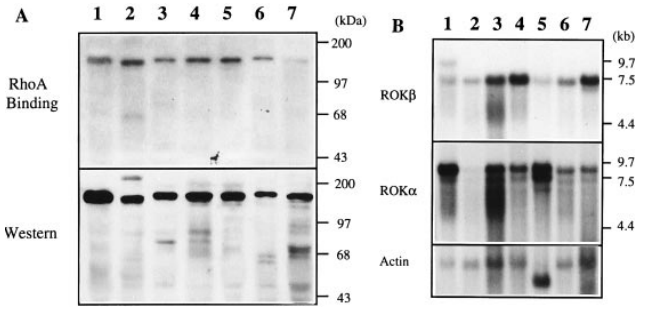

FIG. 2. Expression of ROKs in rat tissues. (A) RhoA binding and Western blotting. Total soluble proteins (150 μg) from rat tissues were separated on a 9% polyacrylamide gel for probing with [γ-^{32}P]GTP-RhoA (upper panel) or polyclonal antibodies raised against ROKα kinase domain (lower panel). Lane 1, brain; lane 2, liver; lane 3, heart; lane 4, kidney; lane 5, lung; lane 6, spleen; lane 7, testis. (B) Northern analysis. The ^{32}P-labeled cDNAs of ROKβ and ROKα were used to probe Northern blots containing poly(A)$^+$ RNA from rat tissues (Clontech). Lane 1, brain; lane 2, spleen; lane 3, lung; lane 4, liver; lane 5, skeletal muscle; lane 6, kidney; lane 7, testis. β-Actin cDNA was used as a control.

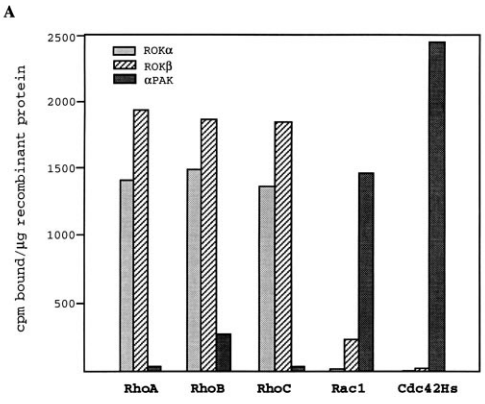

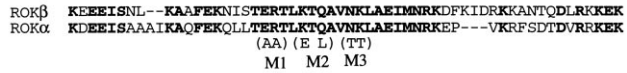

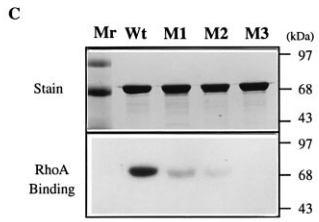

FIG. 3. Specificity of ROK binding. (A) Fusion proteins (1 μg) containing the binding domains of ROKα, ROKβ, and αPAK were dotted onto a nitrocellulose membrane for probing with [γ-^{32}P]GTP-p21. After exposure to X-ray film, radioactive spots were excised for scintillation counting. Results are the means from three determinations. (B) Alignment of the Rho-binding domains of ROKα and ROKβ. The positions of the mutations in mutants M1, M2, and M3 are also indicated. (C) Loss of RhoA binding upon mutation of the binding domain. Fusion proteins of the wild type (Wt) and mutants M1 to M3 (1 μg) were subjected to a [γ-^{32}P]GTP-RhoA binding assay. After washing, the filter was exposed to Hyperfilm for 4 h. For staining, 5 μg of the fusion protein was used. Mr, molecular weight markers.

shown in Fig. 1A. Expression screening of a rat brain cDNA library using RhoA labeled with [γ-^{32}P]GTP also yielded a sequence related to ROKα as well as several RhoA-binding fragments containing overlapping sequences of ROKα. This 1-kb partial cDNA sequence, which encompassed the RhoA-binding site, was then used as a probe in the isolation of overlapping cDNAs encoding the full-length sequence of the related kinase (see Materials and Methods). The cDNA for this new ROK encoded a protein containing 1,369 amino acid residues with a molecular mass of 160 kDa (Fig. 1A). This new Rho-binding kinase, termed ROKβ, has 64% overall identity with ROKα. ROKα and ROKβ contain serine/threonine kinase domains with 90% identity. The region immediately following the kinase domain appears to assume an α-helical coil-coiled structure (data not shown). The kinase domains of ROKα and ROKβ have substantial homology with the myotonic dystrophy kinase (4, 8) and its related family members, including the *warts* gene product of *Drosophila melanogaster* (13) and the fungal *cot-1* gene product (41) (Fig. 1B). Another highly conserved region is the PH domain (27) (Fig. 1C), which interestingly contains a CRD (2) toward the C terminus (Fig. 1D). Conservation of the different domains in ROKα and ROKβ is shown in Fig. 1E.

Antisera raised against the ROKα kinase domain recognized ubiquitous bands of ~160-kDa proteins which generally corresponded to the pattern of RhoA-binding proteins (Fig. 2A). Both methods showed the presence of proteins of different sizes in the various tissues, consistent with kinase heterogeneity. Antibodies raised against the Rho-binding domain of ROKβ recognized the same population of proteins as the antibodies against ROKα kinase domain (data not shown) and were therefore unable to distinguish between the different p160 variants. The cDNAs of ROKα and ROKβ were then used to probe Northern blots containing RNAs from a variety of tissues (Fig. 2B). Using the ROKβ probe, we detected a 7-kb mRNA which was present in all tissues, although at higher levels in the liver, lung, and testis. In the brain, two major bands were found, suggesting that they were products of either alternative splicing or different genes. The ROKα probe detected a major 9-kb mRNA which was enriched in the brain and muscle.

Specificity of p21 binding. Our earlier data indicated that ROKα binds specifically to RhoA and that binding was dependent on the functional state of RhoA (i.e., only the GTP-bound form). RhoA, -B, and -C were all found to bind to the relevant domains of both ROKα and ROKβ. Rac1 and Cdc42Hs were not bound (Fig. 3A). The latter GTPases were bound to the αPAK-binding domain, shown for comparison. Although the overall identity between the binding domains of ROKα and ROKβ was only 60% (Fig. 1E), their alignment revealed a highly conserved stretch of 30 aa, with 20 aa being identical (Fig. 3B). To examine its significance to RhoA binding, mutations were made within this region. The mutants showed loss of RhoA binding, either in great part or totally (Fig. 3C), indicating that this short region is absolutely essential for binding RhoA.

Expression of ROKα promotes formation of stress fibers and focal adhesion complexes. RhoA, either introduced by microinjection or activated by serum growth factors such as lysophosphatidic acid in quiescent fibroblasts, can induce formation of stress fibers and focal adhesion complexes (34). Microinjection of RhoA^{V14} into HeLa cells also resulted in

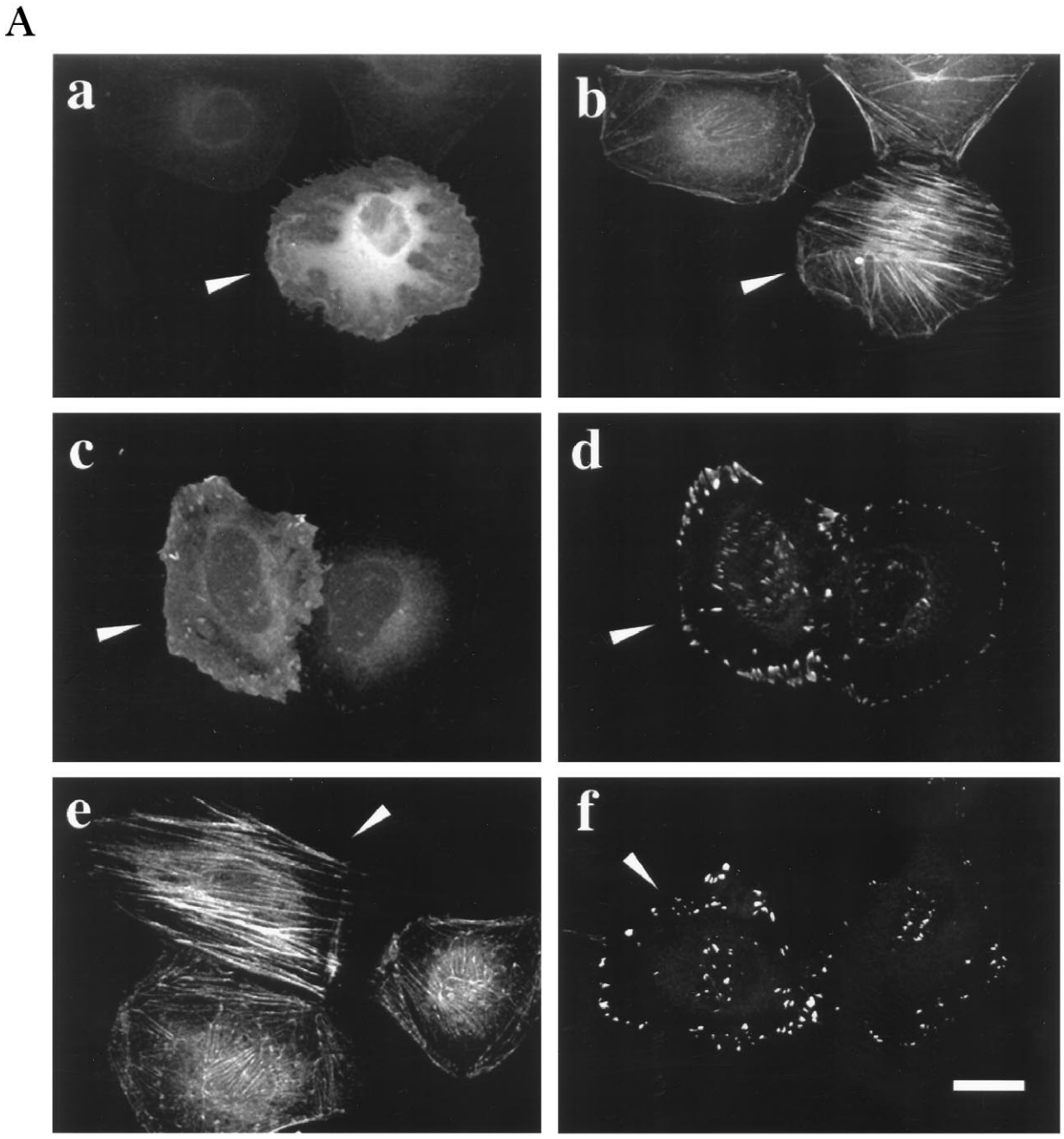

FIG. 4. Overexpression of ROKα promotes formation of stress fibers and adhesion complexes in HeLa cells. (A) HeLa cells grown in serum-free medium for 24 h were microinjected with DNA constructs encoding full-length ROKα (a to d) or C-terminally truncated ROKα$^{1-1271}$ (e and f) and examined 2 h later. All constructs used in this study contained N-terminally HA-tagged sequences (see Materials and Methods). Cells were double stained with anti-HA MAb 12CA5 (a) to detect protein expression and phalloidin (b) to detect filamentous actin or with rhodamine-conjugated anti-HA (c) and antivinculin (d) antibodies to detect focal adhesion complexes. In panels e and f, cells were stained with phalloidin and antivinculin antibody, respectively. Arrowheads point to the injected cells. Confocal images in this and subsequent figures were obtained as described in Materials and Methods. (B) HeLa cells in medium containing 10% FBS were microinjected with DNA constructs encoding full-length ROKα (a and b) or ROKα$^{1-1271}$ (c to h). Cells were stained with anti-HA antibody (a, c, e, and g) and double stained with phalloidin (b and d) or antibodies against vinculin (f) or tubulin (h) 2 h after injection. In this figure and Fig. 8 and 9, expression of constructs is shown on the left, and the cytoskeletal constituents are shown on the right. (C) HeLa cells in medium containing 10% FBS were microinjected with C3 toxin (0.2 μg/μl) and mouse immunoglobulin G (0.5 μg/μl) alone (a to d, arrowheads) or coinjected with either full-length ROKα (a and b, arrows) or ROKα$^{1-1271}$ (c and d, arrows). The cells were stained after 2 h. As controls, cells were also injected with RhoA^{V14} (e, arrowhead) or RhoA^{V14} plus C3 toxin (f, arrowhead) and incubated for 30 min before staining. Cells were double stained with FITC-conjugated anti-mouse antiserum to mark cells injected with C3 (shown on the left) and phalloidin for filamentous actin (shown on the right). Bars = 10 μm.

increased formation of stress fibers; this did not occur in the presence of coinjected C3 toxin (Fig. 4C, e and f). To test whether ROKα had any role in mediating the effects of Rho, we microinjected HeLa cells grown in serum-free medium with plasmid DNA encoding HA-tagged (i) full-length ROKα (containing 1,379 aa), (ii) ROKαK112A mutated in the kinase domain, or (iii) C-terminally truncated ROKα$^{1-1271}$. The expression of the appropriate-size protein from these and other

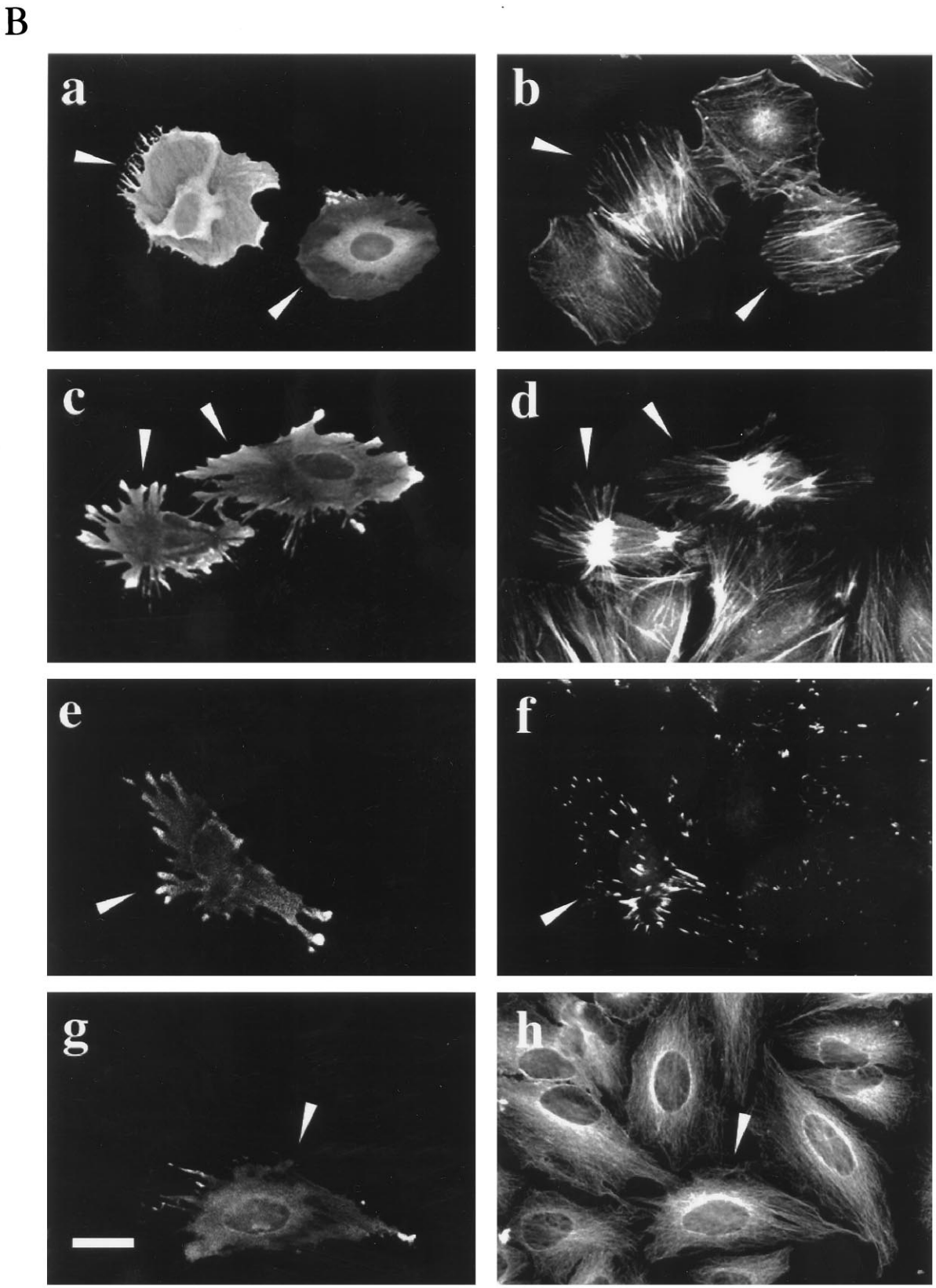

FIG. 4—*Continued.*

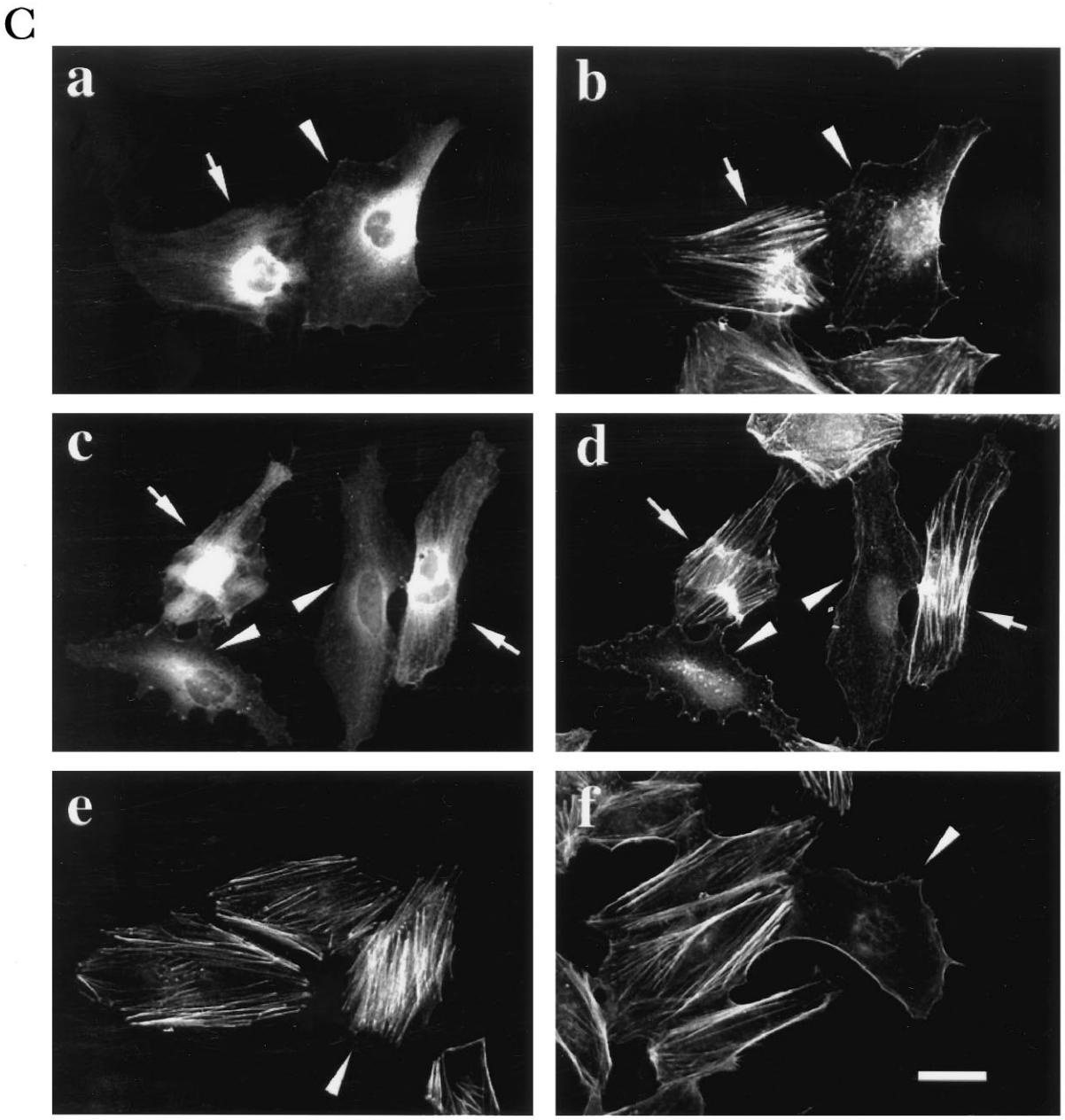

FIG. 4—*Continued.*

constructs used in this study was confirmed by in vitro transcription-translation assay and by analysis of COS-7 cells transfected with these same constructs (see Fig. 9B). Within 1 to 2 h of the injection, stress fibers had formed in cells injected with DNA encoding ROKα (Fig. 4A, a and b), accompanied by increases in vinculin staining (Fig. 4A, c and d), indicative of increased focal adhesion complexes. These effects were not seen in cells injected with cDNA encoding kinase-dead mutant ROKαK112A (Fig. 5). Injection of DNA encoding C-terminally truncated ROKα$^{1-1271}$ resulted in more extensive formation of stress fibers (Fig. 4A, e) and focal adhesion complexes (Fig. 4A, f).

The amount of stress fibers in HeLa cells growing in medium containing 10% FBS (which already contain some stress fibers) could also be increased upon injection of DNA encoding full-length ROKα (Fig. 4B, a and b). Injection of DNA encoding mutant ROK$^{1-1271}$ into these cells again resulted in much more extensive formation of stress fibers. These fibers then appeared to coalesce, leading to a gross condensation of actin filaments within the center of the cell, with some filaments still visibly attached to the cell periphery, and also nuclear disorganization (Fig. 4B, c and d). There were also increased concentrations of focal adhesion complexes (Fig. 4B, e and f). Microtubules were not affected (Fig. 4B, g and h). The effects of both ROKα and ROKα$^{1-1271}$ on stress fiber formation occurred even in the presence of C3 toxin (Fig. 4C, a to d), indicating that these proteins acted downstream of Rho.

To identify the specific domain(s) responsible for the formation of stress fibers and focal adhesion complexes, we tested various mutants of ROKα for their effects on serum-starved

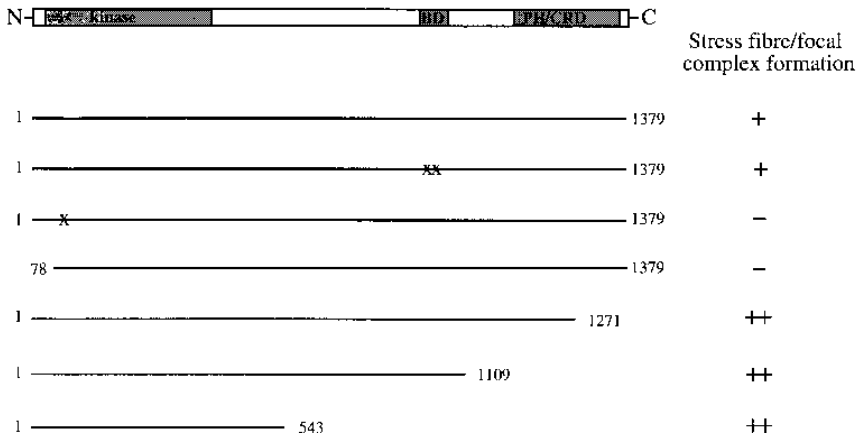

FIG. 5. Analysis of ROKα domains involved in formation of stress fibers and focal adhesion complexes. HeLa cells in serum-free medium were microinjected with DNA constructs encoding ROKα and various mutants. Numbers refer to the N-terminal and C-terminal amino acid residues of the products encoded by the constructs, synthesized as described in Materials and Methods. XX denotes the NK-to-TT mutations (aa 1027 and 1028) in the Rho-binding domain (see Fig. 3C). X marks the position of the K-to-A (aa 112) mutation in the kinase domain. The morphology of the injected cells was analyzed as described for Fig. 4. The effects of the microinjection on formation of stress fibers and focal adhesion complexes are shown on the right, with the relative intensity denoted by the number of plus signs.

cells (Fig. 5). Formation of these cellular structures could be promoted by a short fragment only of ROKα containing the N-terminal portion of kinase domain (i.e., ROKα$^{1-543}$). Both the intact kinase domain and the proximal N-terminal region were required, since ROKαK112A and the N-terminally truncated mutant ROKα$^{78-1379}$ were ineffective in this regard. Under these conditions of overexpression, the RhoA-binding domain was not essential for formation of stress fibers, with the mutants deficient in Rho binding or lacking the binding domain being effective. The C-terminally truncated mutants were all observed to promote formation of more stress fibers and focal adhesion complexes than the full-length ROKα.

The kinase activities of these proteins were analyzed by assaying immunoprecipitated HA-tagged ROKα and mutants from extracts of COS-7 cells transfected with the appropriate DNA constructs. Wild-type (full-length) ROKα exhibited autophosphorylating and kinase activities toward MBP as was previously observed with native ROKα (18). Coexpression with RhoA^{V14} resulted in only a slight increase in ROKα activity (Fig. 6). The ROKαK112A mutant exhibited very little kinase activity, as did the N-terminally truncated mutant ROKα$^{78-1379}$. The N-terminus appears to be essential for kinase activity. On the other hand, the C-terminally truncated ROKα$^{1-1271}$ and ROKα$^{1-543}$ displayed markedly increased kinase activity against MBP. The levels of kinase activities of the various proteins thus appeared to correlate with their morphological effects (Fig. 5).

The N-terminally truncated ROKα$^{78-1379}$ induces loss of stress fibers and focal adhesion complexes. Rather than promoting their formation, we found that the truncated ROKα$^{78-1379}$ induced disappearance of both stress fibers (Fig. 7a and b) and focal adhesion complexes (Fig. 7e and f) upon injection of its DNA. DNA encoding the kinase domain without the N terminus, ROK$^{78-398}$, was ineffective, with the stress fibers (Fig. 7c and d) and focal adhesion complexes (Fig. 7g and h) remaining unaffected. The effect of ROKα$^{78-1379}$ was specific to actin microfilaments, as microtubules were not affected (Fig. 7i and j).

Loss of stress fibers is accompanied by rapid cell spreading. The loss of stress fibers and focal complexes induced by overexpression of ROKα$^{78-1379}$ was accompanied by a rapid increase in cell size, probably as a result of cell flattening and spreading (Fig. 8a and b). These effects were not confined to HeLa cells, as Swiss 3T3 fibroblasts were similarly affected

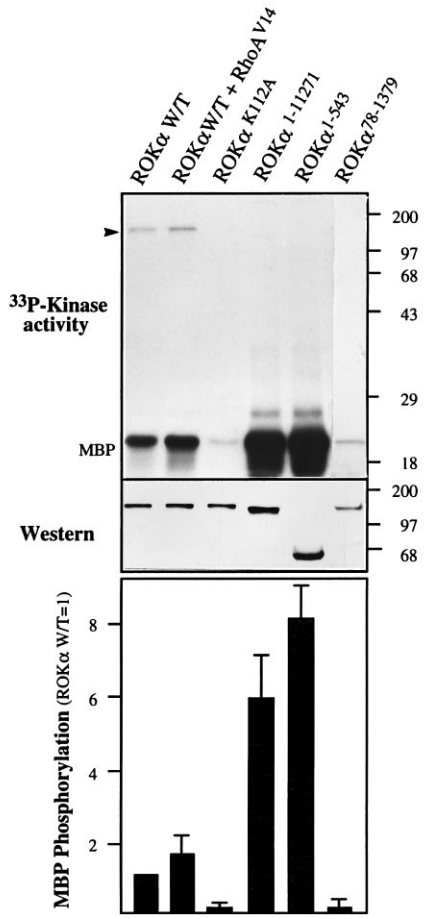

FIG. 6. Protein kinase activities of expressed ROKα and mutants. HA-tagged proteins were immunoprecipitated from COS-7 cells transfected with various HA-tagged DNA constructs. Kinase activity and Western blotting analyses were performed as described in Materials and Methods, using [γ-^{33}P]ATP and a rabbit anti-ROK antibody, respectively. The arrowhead indicates the position of the immunoprecipitated protein. MBP was used as a kinase substrate. In the lower panel, MBP phosphorylation by each construct was determined with a Molecular Dynamics PhosphorImager, and the results are presented as means and standard errors from at least three separate experiments. The activity of wild-type (W/T) ROKα was taken as 1. Sizes are indicated in kilodaltons.

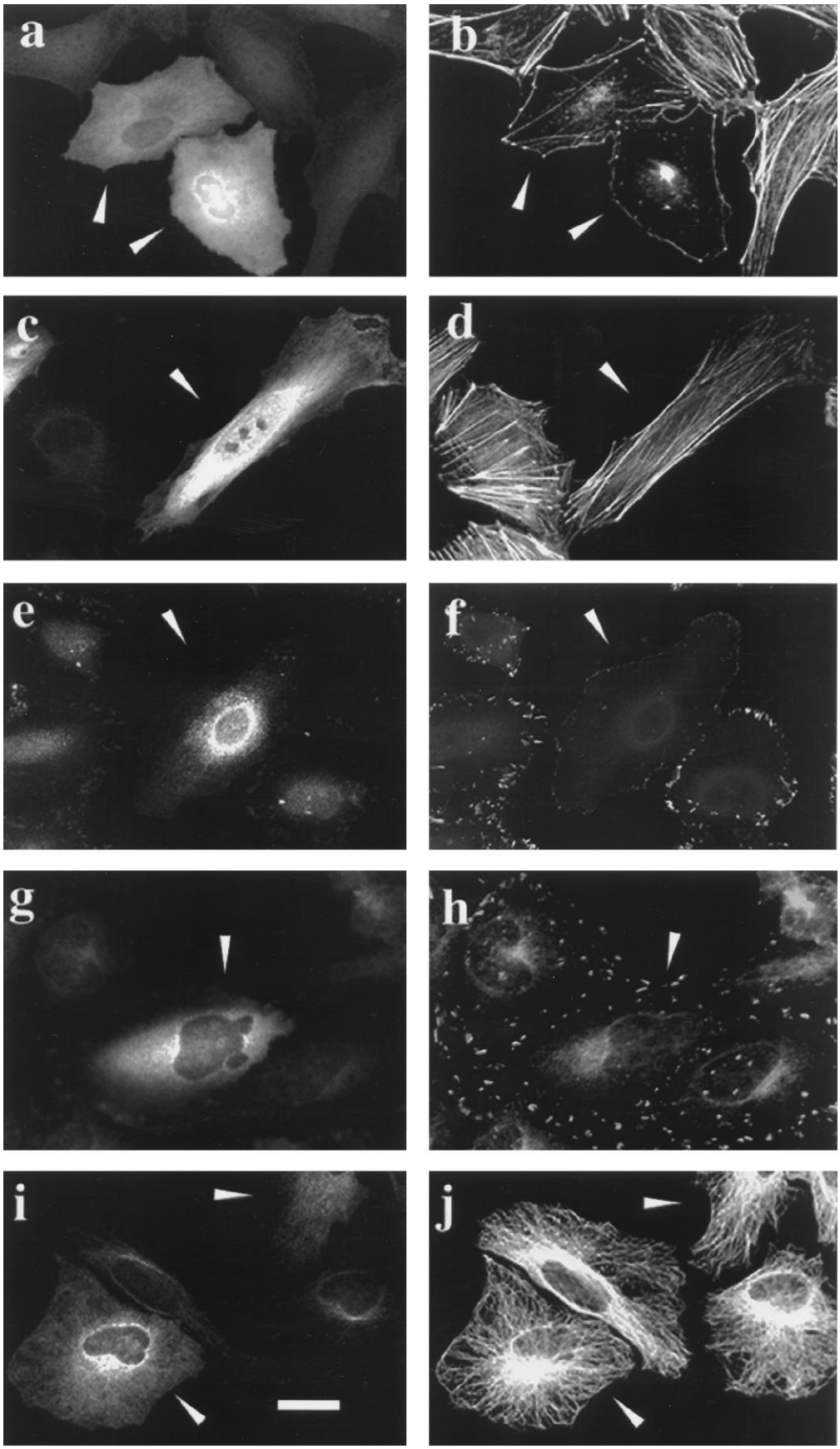

FIG. 7. Effects of overexpression of N-terminally truncated ROKα$^{78\text{-}1379}$ on stress fibers, focal adhesion complexes, and tubulin. HeLa cells in 10% FBS were microinjected with DNA encoding ROKα$^{78\text{-}1379}$ (a, b, e, f, i, and j) and with DNA encoding only kinase domain ROKα$^{78\text{-}398}$ (c, d, g, and h) and examined 2 h later. Protein expression was detected with either MAb 12CA5 (a and c) or rhodamine-conjugated anti-HA antibodies (e, g, and i). Cells were double stained with phalloidin (b and d), antivinculin antibody (f and h), and antitubulin antibody (j). Bar = 10 μm.

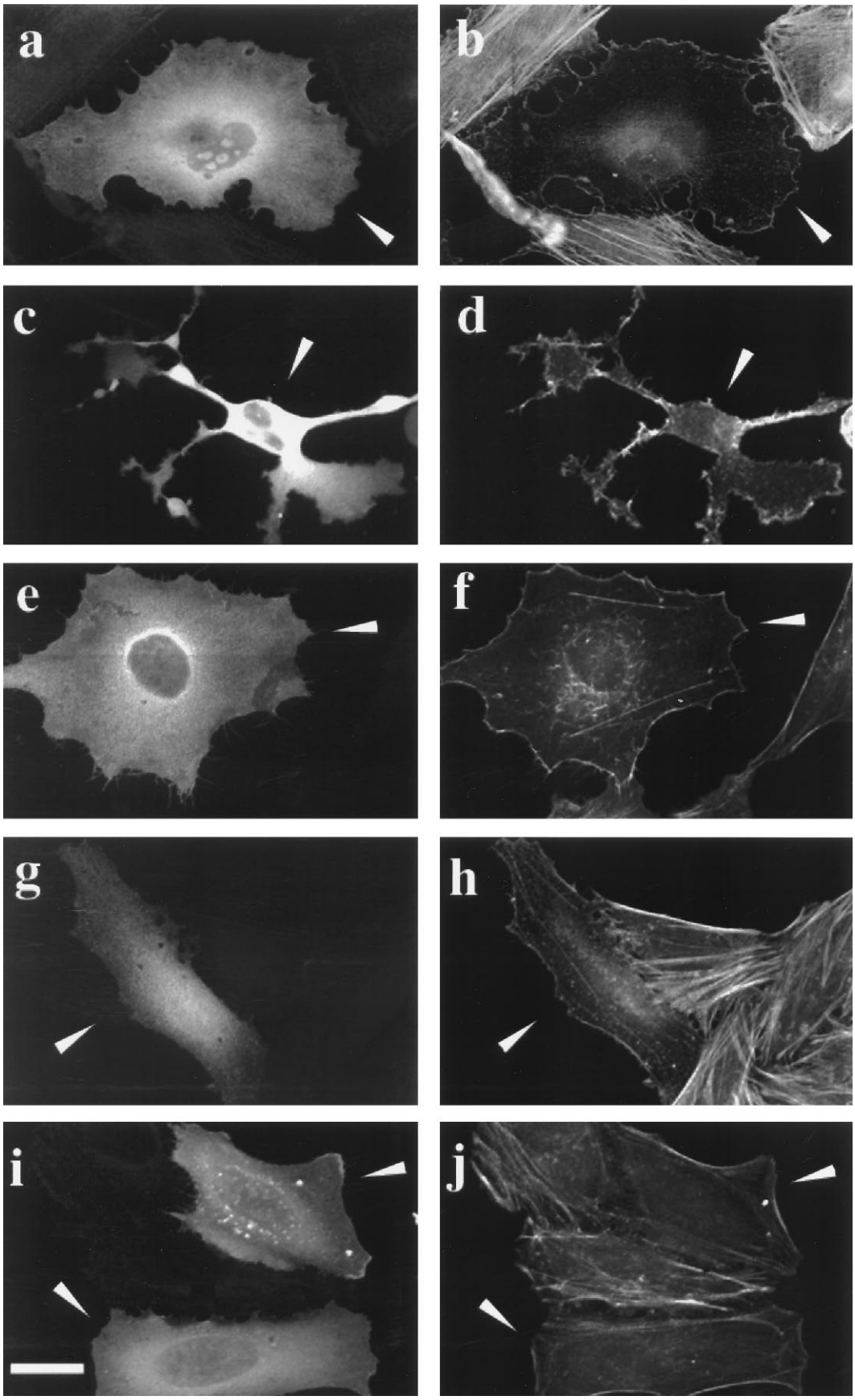

FIG. 8. Overexpression of N-terminally truncated ROKα$^{78\text{-}1379}$ causes cell spreading. HeLa cells in 10% FBS were injected with DNA constructs encoding ROKα$^{78\text{-}1379}$ (a to d), ROKα$^{78\text{-}1379}$ coinjected with Rac1^{N17} cDNA (e to f), C3 transferase and GST (g and h), or RhoA^{N19} (i and j). Expression of ROKα$^{78\text{-}1379}$ and RhoA^{N19} was detected with anti-HA MAb 12CA5 (a, c, e, and i). In panel g, rabbit anti-GST–FITC-conjugated anti-rabbit secondary antibody was used. Cells were fixed 2 h (a, b, e, f, i, and j), 4 h (c and d), or 30 min (cells injected with C3 transferase [g and h]) after injection. Fixed cells were double stained with phalloidin (b, d, f, h, and j). Bar = 10 μm.

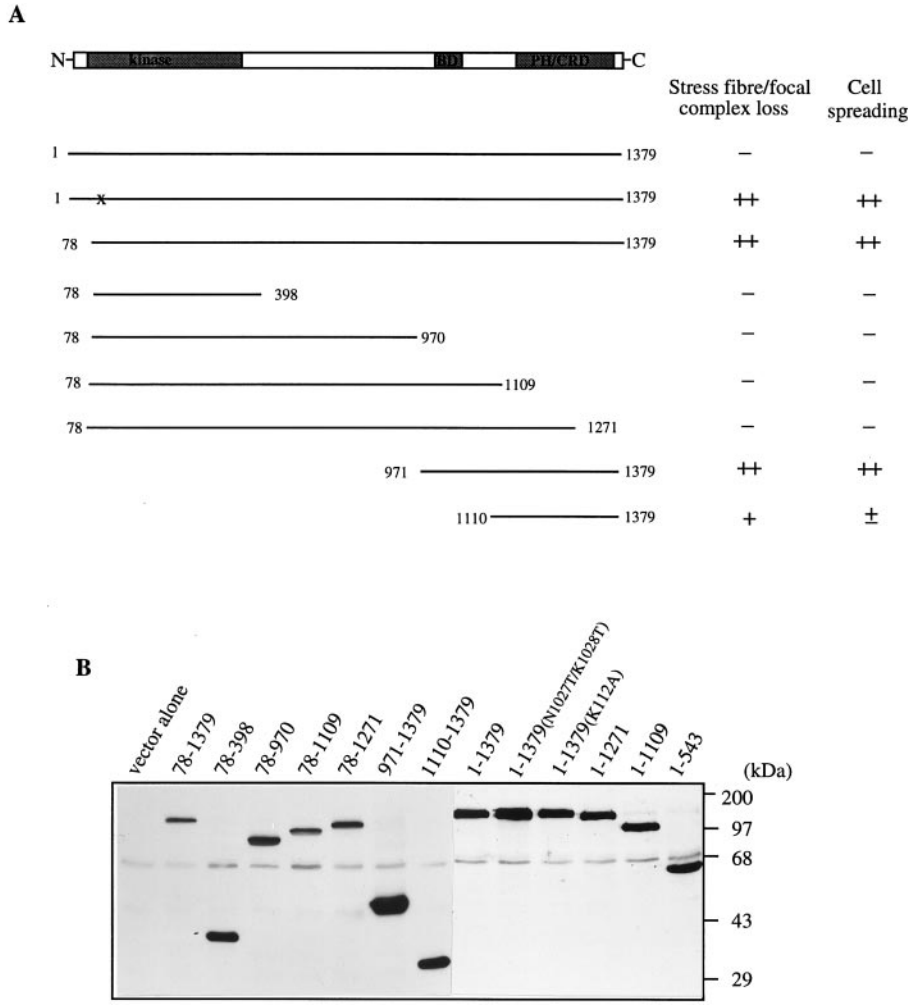

FIG. 9. The PH/CRD motif is responsible for disassembly of stress fibers and focal adhesion complexes and for cell spreading. (A) HeLa cells in 10% FBS were microinjected with DNA constructs encoding ROKα and its mutants. Morphology was analyzed 2 h later as described for Fig. 6. Number designations are as in Fig. 5. Synthesis of the various DNA constructs is described in Materials and Methods. The effects on stress fibers and on cell spreading are summarized on the right, with the relative intensity denoted by increasing the number of plus signs. ± indicates that cell spreading is found in about 50% of the injected cells. (B) Protein expression from various DNA constructs. Plasmid DNA (1 μg) corresponding to constructs shown in panel A was used for transient transfection of COS-7 cells with Lipofectamine (Gibco/BRL). At 16 h after transfection, cells were harvested in lysis buffer and 100-μg aliquots of the soluble extracts were separated on SDS–12% polyacrylamide gels. After transfer onto nitrocellulose, the blot was immunostained with MAb 12CA5. (C) Effects of kinase-dead mutant and C-terminal fragments of ROKα. HeLa cells microinjected with DNA encoding ROKαK112A (a and b), ROKα$^{971-1379}$ (c and d), and ROKα$^{1110-1379}$ (e and f) were stained with either phalloidin (a, c, and e) or antivinculin antibody (b, d, and f) 2 h later. Arrowheads point to the injected cells. Bar = 10 μm.

(result not shown). Prolonged overexpression (3 to 4 h) or transient transfection (results not shown) led to the collapsing of plasma membranes onto the nucleus, resulting in a rounded cell body with irregular branches (Fig. 8c and d). These cells were still viable, as assessed by trypan blue exclusion (data not shown). Because Cdc42Hs, Rac1, and RhoA may operate within a suggested hierarchy (15, 29), the ROKα$^{78-1379}$ mutant, by interfering with normal RhoA function (i.e., formation of stress fibers), could conceivably enhance the function of Rac1, perhaps the GTPase responsible for the cell spreading. This possibility was tested by coinjecting DNAs for truncated ROKα$^{78-1379}$ and for the dominant negative Rac1^{N17} mutant, which blocks the effects of endogenous Rac1 (36). ROKα$^{78-1379}$ still induced cell spreading (Fig. 8e and f), showing that the effect is independent of Rac1. The direct inhibition of Rho by C3 transferase (Fig. 8g and h) and the putative dominant negative RhoA^{N19} mutant (Fig. 8i and j) resulted in stress fiber loss, although only C3 induced some cell spreading.

The PH/CRD motif is essential for loss of stress fibers, loss of focal adhesion complexes, and cell spreading. To determine which particular region of ROKα was involved in inducing loss of the cellular structures and the cell spreading effect, several deletion and point mutation constructs of ROKα were tested. The deletion constructs and a summary of their effects are shown in Fig. 9A. Appropriate-size polypeptides were expressed upon transient transfection of the constructs into COS-7 cells, as detected by antibodies against the HA tag (Fig. 9B) or ROKα (data not shown). Microinjection of these constructs into HeLa cells showed that kinase-dead ROKαK112A induced losses of stress fibers and focal adhesion complexes (Fig. 9C, a and b) as well as the N-terminally truncated ROKα$^{78-1379}$. No such effect occurred if the C terminus was truncated within the PH domain (Fig. 9A, e.g., ROKα$^{78-1271}$). A short fragment containing the C-terminal Rho-binding and PH/CRD motif, ROKα$^{971-1379}$, was extremely effective in inducing the losses (Fig. 9C, c and d) and associated cell spread-

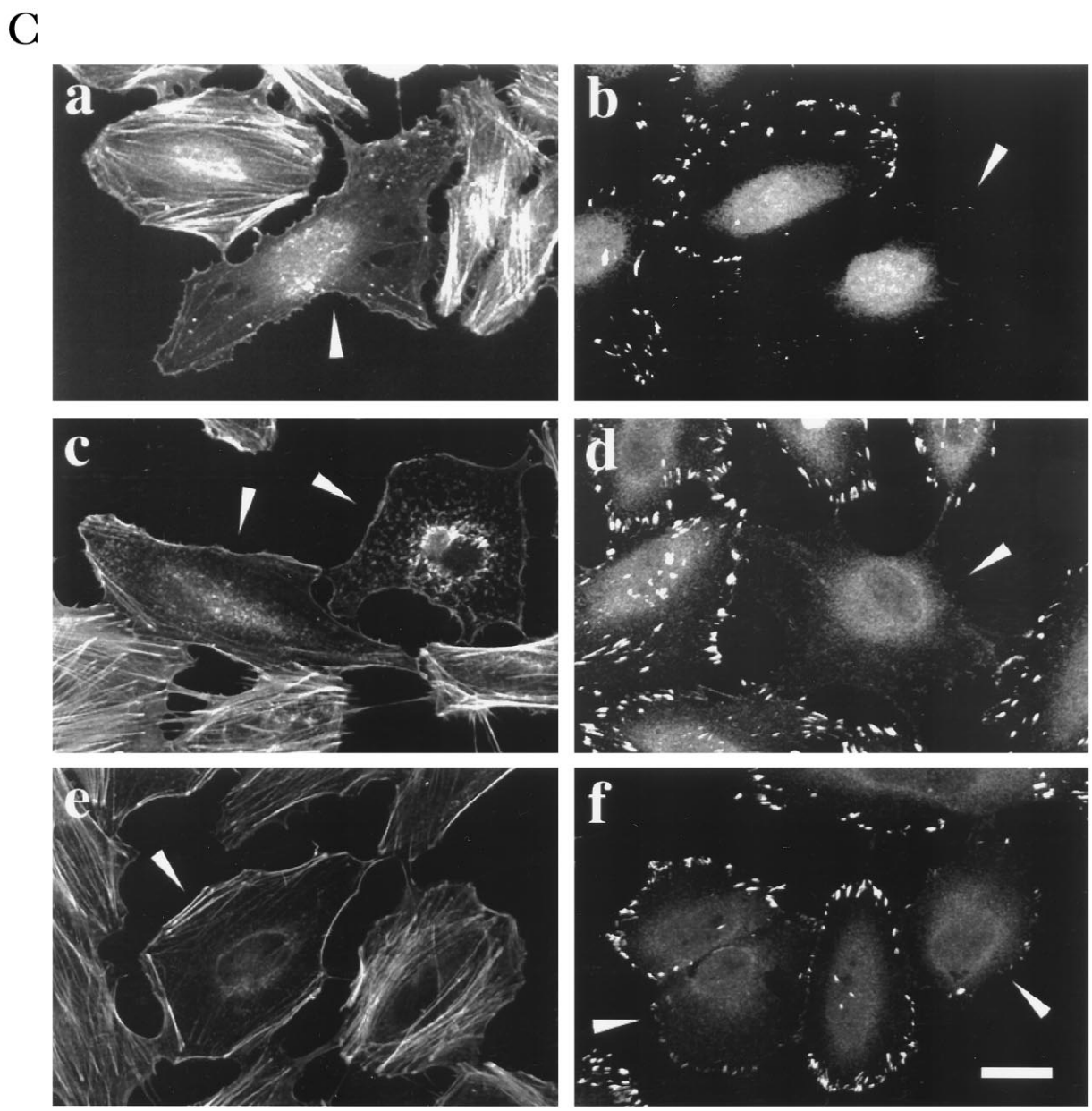

FIG. 9—*Continued.*

ing (Fig. 9A). ROKα$^{1110\text{-}1379}$, containing only the PH/CRD motif, also induced some loss of the structures (Fig. 9B, e and f), but this was accompanied by cell spreading in only about 50% of the injected cells (Fig. 9A).

DISCUSSION

Our earlier work uncovered the presence of ubiquitous proteins of ~150-kDa interacting with RhoA (22). One of these proteins was subsequently isolated and characterized as being a novel serine/threonine kinase termed ROKα (18). From our immunological and mRNA analyses (Fig. 2), we find that the ~150-kDa kinases exist as a heterogenous population, with diverse constituents being present in different tissues, consistent with their being expressed from a number of related genes. The identities and relationship of two of these kinases (ROKα and ROKβ) have now been established through isolation of their cDNAs (Fig. 1). Alignment of the ROKα and ROKβ protein sequences allowed us to pinpoint a short stretch of 20 to 30 aa in both kinases responsible for the interaction with RhoA, -B, and -C. The binding of all three Rho family members is not unexpected, as these p21s have between 85 and 90% sequence identity. Mutational analysis of some critical residues showed this region to be absolutely essential for specific Rho interaction. This region bears no resemblance to the previously reported p21-binding domain of PAK65 and related proteins (22), which specifically interacts with Rac1 and Cdc42 but not RhoA.

These Rho-binding kinases belong to a family of related serine/threonine kinases which includes the myotonic dystrophy kinase, implicated in the etiology of neuromuscular degen-

eration (4, 8) probably as a result of its involvement in ion channel function (26), the fungal *cot-1*-encoded kinase required for controlling filamentous growth (41), and the recently reported *Drosophila* anti-oncogene *warts* gene product, which is essential for controlling cell growth and morphology during development (13). We have also isolated several ~180-kDa proteins containing related kinase domains which do not bind Rho but instead bind Cdc42 and Rac1 (17). In ROKα and ROKβ, there are other highly conserved regions, including the CRD, which lies within the region containing the PH domain, apart from the kinase domain. This family of multidomained ROKs has also been characterized by others (11, 23) whose findings that stimulation of kinase activity toward MBP by RhoA is less than fivefold broadly concur with our results (Fig. 6). This level of GTPase stimulation is very much less than that observed with PAK (19, 22).

Kinase activity appears to be essential for ROKα to promote the formation of stress fibers and focal adhesion complexes. There was a direct relationship between the level of kinase activity and the extent of the morphological effects; mutants lacking kinase activity caused no stress fibers, while mutants exhibiting increased kinase activities promoted more stress fibers than wild-type ROKα (Fig. 5 and 6). However, the hyperactive mutants, e.g., ROKα$^{1\text{-}1271}$, appeared to exert unregulated effects on actin microfilaments, with large-scale formation of stress fibers leading to condensation centrally of actin fibers and also nuclear disorganization. Both the extreme N- and C-terminal regions are necessary for the proper regulation of ROKα kinase and morphological activities, with the N- and C-terminal regions apparently assuming positive and negative regulatory roles, respectively. Thus, N-terminal deletion results in the loss of kinase and stress fiber-forming activities, while C-terminal deletion leads to enhanced kinase activity and greater effects on stress fibers.

In our studies involving the expression of ROKα from introduced DNA, the binding domain did not appear to be essential for ROKα to promote formation of stress fibers and focal adhesion complexes. It is possible that overexpression of exogenous ROKα, which generated an active kinase, had also overridden its need to bind RhoA to function appropriately. Kinase activity is also not substantially increased upon coexpression of activated RhoA^{V14}, which is consistent with RhoA not markedly stimulating native ROK activity in vitro (18). Since introduction of RhoA^{V14} leads to translocation of soluble ROKα to peripheral membranes (18), perhaps in cells expressing normal levels of ROK and Rho, activated Rho is required to direct the kinase to its appropriate destination. In epithelial cells as in fibroblasts, RhoA promotes stress fiber formation which is inhibited by C3 toxin. Nevertheless, prior injection of C3 did not prevent ROKα from promoting stress fibers. However, the kinase-dead ROKαK112A mutant caused loss of stress fibers (present in HeLa cells in 10% FBS) (Fig. 9A and C), behaving as a putative dominant negative inhibitor of endogenous ROK (see below). These results taken together indicate that ROKα acts downstream of Rho in the Rho-dependent pathway of stress fiber formation. The exact role of the Rho-binding domain remains to be established.

The ROKα mutants lacking kinase activity induced morphological changes opposite those promoted by intact ROKα, such as the disassembly of stress fibers and focal adhesion complexes. One plausible explanation is that these mutants interfered with the endogenous ROKs responsible for formation of preexisting stress fibers. This could occur through the mutants acting either as dominant negative mutants (by binding to and blocking the downstream targets of ROKs, e.g., kinase-dead mutant) or as direct inhibitors of the ROKs themselves (e.g., the C-terminal mutants which could act as negative regulators of kinase activity; see above). The C-terminal fragment containing only the PH domain and CRD (both of which have the potential to interact with membranes [2, 9]) induced disassembly. The inclusion of the Rho-binding domain potentiated this effect, perhaps by facilitating the translocation of the inhibitory fragment to peripheral membrane sites (18) where endogenous ROKα operate.

The assembly and disassembly of focal adhesion complexes and concomitant cell spreading have been implicated in migratory activities of squamous cell carcinoma cells (24). Treatment of these cells with hepatocyte growth factor/scatter factor resulted in a biphasic morphological response, with the initial cell spreading being followed by transformation into a spindle-shape phenotype whose motility was sharply increased within 1.5 to 2 h of treatment. This response resembles that elicited with the inhibitory fragments of ROKα, and it would be of interest to determine if inhibition of ROKs which are ubiquitous precedes cell spreading and whether cell spreading of the squamous cells and that induced in HeLa cells are related events. In addition to ROKα, other kinases such as the tyrosine kinases downstream of Rho (35) participate in the formation of stress fibers and focal adhesion complexes. Some of the morphological effects of other Rho family members are exerted through nuclear events (7, 10, 25) which are mediated by kinase cascades. Thus, in the yeast pheromone mating pathway, Cdc42 participates in the mitogen-activated protein kinase pathway (37, 44). In mammalian cells, Rac1 and Cdc42 are linked to the c-JNK/mitogen-activated protein kinase cascade (7, 25), while RhoA appears to be involved in a separate nuclear event leading to the activation of a serum-responsive factor-linked pathway (10). The specific interaction of ROKs with RhoA, -B, and -C only in their GTP-bound forms and the ability of ROKα to promote stress fiber formation are consistent with these kinases being target and effector proteins. The presence of multiple domains in ROKs capable of interacting with other signalling and cytoskeletal components (and some perhaps having discrete functions) clearly endows them with the ability to mediate the various roles of the Rho GTPases in cellular functions as diverse as apoptosis (12) and transformation (32).

ACKNOWLEDGMENTS

We thank Lydia Tan, Ivan Tan, and Ivy Ho for expert technical assistance; Ben Li for oligonucleotide synthesis; and Francis Leong for photographic reproduction.

This work was supported by the Glaxo Singapore Research Fund.

REFERENCES

1. **Adamson, P., H. F. Paterson, and A. Hall.** 1992. Intracellular localization of the p21rho proteins. J. Cell Biol. **119:**617–627.
2. **Ahmed, S., R. Kozma, J. Lee, C. Monfries, N. Harden, and L. Lim.** 1991. The cysteine-rich domain of human proteins, neuronal chimaerin, protein kinase C and diacylglycerol kinase binds zinc. Biochem. J. **280:**233–241.
3. **Bowman, E. P., D. J. Uhlinger, and J. D. Lambeth.** 1993. Neutrophil phospholipase D is activated by a membrane-associated Rho family small molecular weight GTP-binding protein. J. Biol. Chem. **268:**21509–21512.
4. **Brook, J. D., M. E. McCurrach, H. G. Harley, A. J. Buckler, D. Church, H. Aburatani, K. Hunter, V. P. Stanton, J.-P. Thirion, T. Hudson, R. Sohn, B. Zemelman, R. G. Snell, S. A. Rundle, S. Crow, J. Davies, P. Shelbourne, J. Buxton, C. Jones, V. Juvonen, K. Johnson, P. S. Harper, D. J. Shaw, and D. E. Housman.** 1992. Molecular basis of myotonic dystrophy: expansion of a trinucleotide (CTG) repeat at the 3′ end of a transcript encoding a protein kinase family member. Cell **68:**799–808.
5. **Chardin, P., P. Madaule, and A. Tavitian.** 1988. Coding sequence of human *rho* cDNAs clone 6 and clone 9. Nucleic Acids Res. **16:**2717.
6. **Chong, L. D., A. Traynor-Kaplan, G. M. Bokoch, and M. A. Schwartz.** 1994. The small GTP-binding protein Rho regulates a phosphatidylinositol 4-phosphate 5-kinase in mammalian cells. Cell **79:**507–513.
7. **Coso, O. A., M. Chearillo, J.-C. Yu, H. Teramoto, P. Crespo, N. Xu, T. Miki,**

and J. S. Gutkind. 1995. The small GTP-binding protein Rac1 and Cdc42 regulate the activity of the JNK/SAKP signaling pathway. Cell **81:**1137–1146.
8. **Fu, Y.-H., A. Pizzuti, R. G. Fenwick, Jr., J. King, S. Rajnarayan, P. W. Dunne, J. Dubel, G. A. Nasser, T. Ashizawa, P. de Jong, B. Wieringa, R. Korneluk, M. B. Perryman, H. F. Epstein, and C. T. Caskey.** 1992. An unstable triplet repeat in a gene related to myotonic muscular dystrophy. Science **255:**1256–1258.
9. **Harlan, J. E., H. S. Yoon, P. J. Hajduk, and S. W. Fesik.** 1995. Structural characterization of the interaction between a pleckstrin homology domain and phosphatidylinositol 4,5-bisphosphate. Biochemistry **34:**9859–9864.
10. **Hill, C. S., J. Wynne, and R. Treisman.** 1995. The Rho family GTPases RhoA, Rac1, and Cdc42Hs regulate transcriptional activation by SRF. Cell **81:**1159–1170.
11. **Ishizaki, T., M. Maekawa, K. Fujisawa, K. Okawa, A. Iwamatsu, A. Fujita, N. Watanabe, Y. Saito, A. Kakizuka, N. Morii, and S. Narumiya.** 1996. The small GTP-binding protein Rho binds to and activates a 160 kDa Ser/Tre protein kinase homologous to myotonic dystrophy kinase. EMBO J. **15:** 1885–1893.
12. **Jimenez, B., M. Arends, P. Esteve, R. Perona, R. Sanchez, S. R. Cahal, A. Wyllie, and J. C. Lacal.** 1995. Induction of apoptosis in NIH3T3 cells after serum deprivation by overexpression of rho-p21, a GTPase protein of the ras superfamily. Oncogene **10:**811–816.
13. **Justice, R. W., O. Zilian, D. F. Woods, M. Noll, and P. J. Bryant.** 1995. The drosophila tumour suppressor gene *warts* encodes a homolog of human myotonic dystrophy kinase and is required for the control of cell shape and proliferation. Genes Dev. **9:**534–546.
13a. **Kaibuchi, K., and S. Narumiya.** Personal communication.
14. **Kishi, K., T. Sasaki, S. Kuroda, T. Itoh, and Y. Takai.** 1993. Regulation of cytoplasmic division of *Xenopus* embryo by rhop21 and its inhibitory GDP/GTP exchange protein (rho GDI). J. Cell Biol. **120:**1187–1195.
15. **Kozma, R., S. Ahmed, A. Best, and L. Lim.** 1995. The Ras-related protein Cdc42Hs and bradykinin promote formation of peripheral actin microspikes and filopodia in Swiss 3T3 fibroblasts. Mol. Cell. Biol. **15:**1942–1952.
16. **Leung, T., B.-E. How, E. Manser, and L. Lim.** 1993. Germ cell β-chimaerin, a new GTPase-activating protein for p21*rac*, is specifically expressed during the acrosomal assembly stage in rat testis. J. Biol. Chem. **268:**3813–3816.
17. **Leung, T., E. Manser, and L. Lim.** Unpublished data.
18. **Leung, T., E. Manser, L. Tan, and L. Lim.** 1995. A novel serine/threonine kinase binding the ras-related RhoA GTPase which translocates the kinase to peripheral membranes. J. Biol. Chem. **256:**29051–29054.
19. **Manser, E., C. Chong, Z.-S. Zhao, T. Leung, G. Michael, C. Hall, and L. Lim.** 1995. Molecular cloning of a new member of the p21-Cdc42/Rac-activated kinase (PAK) family. J. Biol. Chem. **270:**25070–25078.
20. **Manser, E., T. Leung, C. Monfries, M. Teo, C. Hall, and L. Lim.** 1992. Diversity and versatility of GTPase activating proteins for the p21rho subfamily of ras G proteins detected by a novel overlay assay. J. Biol. Chem. **267:**16025–16028.
21. **Manser, E., T. Leung, H. Salihuddin, L. Tan, and L. Lim.** 1993. A non-receptor tyrosine kinase that inhibits the GTPase activity of p21cdc42. Nature (London) **363:**364–367.
22. **Manser, E., T. Leung, H. Salihuddin, Z.-S. Zhao, and L. Lim.** 1994. A brain serine/threonine protein kinase activated by Cdc42 and Rac1. Nature (London) **367:**40–46.
23. **Matsui, T., M. Amano, T. Yamamoto, K. Chihara, M. Nakafuku, M. Ito, T. Nakano, K. Okawa, A. Iwamatsu, and K. Kaibuchi.** 1996. Rho-associated kinase, a novel serine/threonine kinase, as a putative target for the small GTP binding protein Rho. EMBO J. **15:**2208–2216.
24. **Matsumoto, K., K. Matsumoto, T. Nakamura, and R. H. Kramer.** 1994. Hepatocyte growth factor/scatter factor induces tyrosine phosphorylation of focal adhesion kinase ($p125^{FAK}$) and promotes migration and invasion by oral squamous cell carcinoma cells. J. Biol. Chem. **269:**31807–31813.
25. **Minden, A., A. Lin, F.-X. Claret, A. Abo, and M. Karin.** 1995. Selective activation of the JNK signaling cascade and c-Jun transcriptional activity by the small GTPases Rac and Cdc42Hs. Cell **81:**1147–1157.
26. **Mounsey, J. P., P. Xu, J. E. John, L. T. Horne, J. Gilbert, A. D. Roses, and J. R. Moorman.** 1995. Modulation of skeletal muscle sodium channels by human myotonin protein kinase. J. Clin. Invest. **95:**2379–2384.
27. **Musacchio, A., T. Gibson, P. Rice, J. Thompson, and M. Saraste.** 1993. The PH domain: a common piece in the structural patchwork of signalling proteins. Trends Biochem. Sci. **19:**343–348.
28. **Nishiyama, T., T. Sasaki, K. Takaishi, M. Kato, H. Yaku, K. Araki, Y. Matsuura, and Y. Takai.** 1994. *rac* p21 is involved in insulin-induced membrane ruffling and *rho* is involved in hepatocyte growth factor- and 12-*O*-tetradecanoylphorbol-13-acetate-induced membrane ruffling in KB cells. Mol. Cell. Biol. **14:**2447–2456.
29. **Nobes, C. D., and A. Hall.** 1995. Rho, Rac, and Cdc42 GTPases regulate the assembly of multimolecular focal complexes associated with actin stress fibers, lamellipodia, and filopodia. Cell **81:**53–62.
30. **Paterson, H. F., A. J. Self, M. D. Garrett, I. Just, K. Atkories, and A. Hall.** 1990. Microinjection of recombinant $p21^{rho}$ induces rapid change in cell morphology. J. Cell Biol. **111:**1001–1007.
31. **Perona, R., P. Esteve, B. Jimenez, R. P. Ballestero, S. R. Cajal, and J. C. Lacal.** 1993. Tumorigenic activity of rho genes from *Aplysia california*. Oncogene **8:**1285–1292.
32. **Prendergast, G. C., R. Khosravi-Far, P. A. Solske, H. Kurzawa, P. F. Lebowitz, and C. J. Der.** 1995. Critical role of Rho in cell transformation by oncogenic Ras. Oncogene **10:**2289–2296.
33. **Ridley, A. J.** 1995. Rho-related proteins: actin cytoskeleton and cell cycle. Curr. Opin. Genet. Dev. **5:**24–30.
34. **Ridley, A. J., and A. Hall.** 1992. The small GTP-binding protein rho regulates the assembly of focal adhesion and actin stress fibres in response to growth factors. Cell **70:**389–399.
35. **Ridley, A. J., and A. Hall.** 1994. Signal transduction pathways regulating rho-mediated stress fiber formation: requirement for a tyrosine kinase. EMBO J. **13:**2600–2610.
36. **Ridley, A. J., H. F. Paterson, C. L. Johnston, D. Diekmann, and A. Hall.** 1992. The small GTP-binding protein rac regulates growth factor induced membrane ruffling. Cell **70:**401–410.
37. **Simon, M.-N., C. de Virgillo, B. Souza, J. R. Pringle, A. Abo, and S. I. Reed.** 1995. Role for the Rho-family GTPase Cdc42 in yeast mating pheromone signal pathway. Nature (London) **376:**702–705.
38. **Takai, Y., T. Sasaki, K. Tanaka, and H. Nakanishi.** 1995. Rho as a regulator of the cytoskeleton. Trends Biochem. Sci. **20:**227–231.
39. **Takaishi, K., A. Kikuchi, S. Kuroda, K. Kotani, T. Sasaki, and Y. Takai.** 1993. Involvement of rhop21 and its inhibitory GDP/GTP exchange protein (rhoGDI) in cell motility. Mol. Cell. Biol. **13:**72–79.
40. **Xiao, J. H., I. Davidson, H. Matthes, J.-M. Garnier, and P. Chambon.** 1991. Cloning, expression and transcriptional properties of the human enhancer factor TEF-1. Cell **65:**551–568.
41. **Yarden, O., M. Plamann, D. J. Ebbole, and C. Yanofsky.** 1992. *cot-1*, a gene required for hyphal elongation in *Neurospora crassa*, encodes a protein kinase. EMBO J. **11:**2159–2166.
42. **Zalcman, G., V. Glosson, G. Linares-Cruz, F. Lerebours, N. Hovore, A. Taritain, and B. Olofsson.** 1995. Regulation of ras-related RhoB protein expression during the cell cycle. Oncogene **10:**1935–1945.
43. **Zhang, J., W. G. King, S. Dillon, A. Hall, L. Feig, and S. E. Rittenhouse.** 1993. Activation of platelet phosphatidylinositide 3-kinase requires the small GTP-binding protein Rho. J. Biol. Chem. **268:**22251–22254.
44. **Zhao, Z.-S., T. Leung, E. Manser, and L. Lim.** 1995. Pheromone signalling in *Saccharomyces cerevisiae* requires the small GTP-binding protein Cdc42p and its activator CDC24. Mol. Cell. Biol. **15:**5246–5257.